Proceedings of the IEEE Workshop on Statistical and Computational Theories of Vision, Fort Collins, CO, June, 1999. (Published on Web).

Graded Learning for Object Detection

Francois Fleuret[1] and Donald Geman[2]

Abstract

Our goal is to detect all instances of a generic object class, such as a face, in greyscale scenes. The design of the algorithm is motivated by computational efficiency. The search is coarse-to-fine in both the exploration of poses and the representation of the object class. Starting from training examples, we recursively learn a hierarchy of spatial arrangements of edge fragments, graded by their size (sparsity). The arrangements have no a priori semantic or geometric interpretation. Instead, they are selected to be "decomposable": Each can be split into two correlated subarrangements, each of which can be further divided, etc. As a result, the probability of an arrangement of size k appearing on an object instance decays slowly with k. We demonstrate this both theoretically and in experiments in which detection means finding a sufficient number of arrangements of various sizes.

1. Avant-Projet IMEDIA, INRIA-Rocquencourt, Domaine de Voluceau, B.P.105, 78153 Le Chesnay. Supported in part by the CNET.

2. Department of Mathematics and Statistics, University of Massachusetts, Amherst, MA 01003; Supported in part by the ONR under contract N00014-97-1-0249 and the ARO under MURI grant DAAH04-96-1-0445.

1 Introduction

Starting with a training set of examples of a generic object class (e.g., "face"), our goal is to construct an algorithm to detect and localize all instances of this class in greyscale scenes. The examples are subimages containing a single instance of the object at various poses, for example frontal views of faces at a range of scales, tilts, etc. Whereas the "backgrounds" in the training samples might be very simple, the detection algorithm must function in natural, highly cluttered scenes. We measure performance by the false alarm rate and the size of the training set necessary to achieve a very small false negative rate.

This work belongs to an ongoing and broader project on visual recognition as a "twenty questions game" - a problem in efficient coding. We design features (image functionals) and search strategies at the same time and in a highly coarse-to-fine manner in both (i) the density of the object representations and (ii) the exploration of the space of poses. This paradigm was analyzed in the context of decision trees and stepwise uncertainty reduction in [2], [8], [9] and [16]. Although the approach to learning is different here, and no trees are induced, the final algorithm can be expressed as a huge, recursively coded tree of binary "queries" based on comparisons of intensity differences.

We learn a hierarchy of increasingly complex features. In order to declare detections, we successively check for a minimal number of each complexity. As in [3], the features are binary image functionals corresponding to the presence or absence of spatial arrangements of edge fragments. The fragments have an approximate location and an approximate orientation; the definition is purposely loose in order to accommodate geometric invariance. The arrangements have no a priori semantical or geometric interpretation. Instead, we simply want them to be as likely as possible on the object class. Specificity alone renders them rare in general backgrounds.

We introduce the notion of a "decomposable arrangement" and as well as an algorithm for discovering large numbers of these from training examples. This is the main contribution of the paper. "Decomposable" means that the arrangement can be divided into two highly correlated subarrangements, each of which further splits into two highly correlated smaller arrangements, and so forth all the way down the individual edge fragments. The learning algorithm is a procedure for building larger and larger arrangements in a recursive, bottom-up fashion. The motivation is that the probability of an decomposable arrangement of size k appearing on an object instance decreases very gradually as k increases, thus insuring features which are highly discriminating in separating objects from background. This statement will be justified theoretically and illustrated empirically.

In order to emphasize the new ideas and the statistical learning framework we shall only apply the learning algorithm to training examples in one particular subset of poses. The pose of a face means the shape and location of the triangle formed by the two eyes and the mouth. We will indicate how exactly the same routine is repeatedly applied to a series of successively more constrained learning sets (groups of triangles) in order to detect faces over a wide range of presentations; details and experiments are in [7]. In the end the processing is coarse-to-fine in both the subdivisions of pose space and the search for successively denser arrangements. The predecessor of this approach, demonstrated in [3], is to train at a single reference pose and then relax the geometrical constraints to accommodate other poses, using a generalized Hough transform to minimize computation.

Two experiments are described. One is synthetic - detecting "wings" in a world of lines. It is very challenging because, by design, the wings are locally indistinguishable from the "clutter" (diagonal lines). The other experiment is real - detecting frontal views of faces. We use the Olivetti training set of 300 faces: 10 pictures of each of 30 individuals. A relatively small training is sufficient since we only use it to estimate correlations, and training only requires a few minutes on a PC. In particular, we do not estimate a large system of coupled parameters as in other statistical learning methods. Also, invariance and other properties are largely "hard-wired" rather than learned.

2 Invariant Object Detection

The problem of detecting instances from a generic object class without information due to color, depth or motion has been widely studied in the computer vision literature. For example, in the case of faces, a variety of methods have been proposed, including artificial neural networks [12], [13], support vector machines [11], graph-matching [10], Bayesian inference [5], deformable templates [17], and the precursors of our methodology already cited.

One of the principal difficulties is the variation in the appearance of faces due to the vagaries of lighting; see for example the discussion in [14]. Our approach is to build a large degree of photometric invariance into the definition of the edge fragments by considering only comparisons of intensity differences; see Section 4. Similarly, our approach to geometric invariance is quite explicit. Each arrangement is a conjunction of elementary tests, which are themselves disjunctions of edge fragments; we then compare the number of arrangements present to a threshold. Detection is then finally based on a massive disjunction of conjunctions of highly localized edge fragments, a very literal treatment of geometric invariance and in sharp contrast to most other approaches; see [3] for a more complete discussion.

3 Statistical Framework

Let $\mathcal{I}$ denote the set of (sub)images $I = \{I(x), x \in R\}$, where R is a reference grid (e.g., 32×32) and $I(x)$ is quantized in a standard way, say to 256 grey levels. The subimages are divided into two categories - "object" and "background." The object pictures contain a single instance of the object class at a reference pose, meaning that the object is roughly centered in the subimage and the scale of the object is roughly that of the grid R. The background pictures are everything else. Let $Y(I) \in \{0, 1\}$ stand for the class of I with "0" corresponding to background.

Let P denote a probability measure on $\mathcal{I}$. We can think of P as the empirical measure on all subimages of all images in some large database. Then P induces two conditional measures: $P_0(.) = P(.|Y = 0)$, the distribution on the background class and $P_1(.) = P(.|Y = 1)$, the distribution on the object class. Given a classifier $f : \mathcal{I} \to \{0, 1\}$, the false negative error rate is $\alpha(f) = P_1(f = 0)$ and the false positive error rate is $\beta(f) = P_0(f = 1)$. Ideally, we seek to minimize $\beta(f)$ subject to $\alpha(f) = 0$; this is part of the motivation for the classifier we define in Section 5.

The training set $\mathcal{L}$ is assumed to be a random sample from $\mathcal{I}$ under P_1. We use negative examples (i.e., samples from P_0) to estimate false alarm rates but not to construct the classifier. An important constraint is that the size of $\mathcal{L}$ is not sufficiently large to reliably estimate a number of *inter-dependent* parameters of the same order. Moreover, whereas the training set is a genuine random sample in the synthetic problem, this will rarely be the case in real problems.

Since our approach is inductive rather than deductive, we do not propose a *model* for either P_0 or P_1; instead, we rely on the empirical measure $\hat{P}_1$ induced from $\mathcal{L}$. Thus, we define a classifier directly from $\mathcal{L}$. By and large, training then amounts to estimating the probability distribution under P_1 of events in $\mathcal{I}$; these probabilities determine the components of the classifier and are derived by relative frequencies in $\mathcal{L}$. Another possibility would be to estimate *both* P_0 and P_1 and take corresponding the maximum likelihood classifier, but this appears to be impractical; the background distribution is extremely difficult to model and computing the maximum likelihood estimator is only feasible in simple cases.

4 A Hierarchy of Features

We seek a coarse-to-fine hierarchy of features, ranging from primitive (sparse and local) to complex (dense and global), whose statistics in the two populations become increasingly disparate. Computational efficiency is achieved by progressively checking for more and more complex attributes in order to separate instances of clutter from instances of object. Many subimages can be immediately dismissed as object candidates based on the primitive features, such as edge counts; more global confusions will require further examination involving higher-order correlations and longer-range dependencies.

4.1 Elementary Tests

All our features are conjunctions of *binary, elementary tests*. The elementary tests are local disjunctions of localized filters. In our experiments the local filters detect edge fragments; other, more sophisticated, filters might be more effective. Each edge filter is applied at each location in R, and has an orientation (horizontal or vertical) and a polarity (plus or minus). Consider a horizontal edge of positive polarity at location x. This means that $I(x) > I(x')$, where x and x' are vertical neighbors, and that $I(x) - I(x') > \max_y\{|I(x) - I(y)|, |I(x') - I(y)|\}$ for a certain number of neighboring pixels y. In Figure 6 we show a training face (left) together with the detected edge fragments (middle).

There is one elementary test $X_i = X_i(I)$ for each edge fragment, $i = 1, 2, ..., d$, where $d \approx 4|R|$. Test $X_i = 1$ if the corresponding edge is present in a small neighborhood of x_i and $X_i = 0$ otherwise. The size of the neighborhood (the degree of "floating") depends on the subset in pose space that defines the learning problem; it is chosen to make the probability of the elementary tests of order $\frac{1}{2}$.

4.2 Decomposable Arrangements

We refer to a subset $A \subset \{1, \ldots, d\}$ as an *arrangement*; the corresponding random variable

$$X_A(I) = \prod_{i \in A} X_i(I)$$

on $\mathcal{I}$ is simply a spatial conjunction of elementary tests: $X_A = 1$ if and only if $X_i = 1$ for each $i \in A$. Let $suppX_i \subset R$ be the set of pixels which appear in the definition of X_i. In order to limit the family of arrangements we shall assume that $suppX_i \bigcap suppX_j = \emptyset$ whenever $i, j \in A$ and $i \neq j$. We write $|A|$ for the size of A. This is our pool of features; the classifier will be constructed from a subset of these.

We want to find arrangements A for which the statistics of X_A are as different as possible under P_0 and P_1. Since estimation under P_0 is problematic, we will attempt to obtain the desired disparity by constructing arrangements which are large but still likely under P_1. Size alone renders them rare under P_0. The construction is based on correlation. Let $\rho(U, V)$ denote the correlation coefficient of random variables U and V with respect to P_1. For binary variables with $0 < P_1(U = 1), P_1(V = 1) < 1$ we have

$$\rho(U, V) = \frac{P_1(U = 1, V = 1) - P_1(U = 1)P_1(V = 1)}{(P(U = 1)P(U = 0)P(V = 1)P(V = 0))^{1/2}}.$$

Consider arrangements X_iX_j of size two. We could filter all such pairs by requiring that $\rho(X_i, X_j) \geq \rho$ for some threshold ρ, $0 < \rho < 1$. This yields pairs of elementary tests which tend to occur (or not occur) together on objects. Similarly, $X_iX_jX_k$ might be a good candidate for a discriminating arrangement of size three if, in addition, $\rho(X_iX_j, X_k) \geq \rho$. Continuing in this way, we can single out arrangements of size four by combining two "good" pairs X_iX_j and X_kX_l and further requiring that $\rho(X_iX_j, X_kX_l) \geq \rho$. And so forth.

Define a *decomposition* of A to be any nested set of binary partitions (i.e., successive binary refinements) all the way down to individual elements of $\{1, 2, ..., d\}$. We shall also assume that a partition cell splits evenly if its size is even and splits into two child cells whose sizes differ by exactly one if its size is odd. Call it a *ρ-decomposition* if the correlation inequality holds at every split. In Figure 1 we show one decomposition of $A = \{1, 2, 4, 5, 9\}$. It is a ρ-decomposition if $\rho(X_1X_4,\ X_2X_5X_9) \geq \rho$, $\rho(X_1,\ X_4) \geq \rho$, $\rho(X_5X_9,\ X_2) \geq \rho$ and $\rho(X_5,\ X_9) \geq \rho$. Finally, an arrangement A, or the corresponding random variable X_A, will be called *ρ-decomposable* if there is *at least one* ρ- decomposition of A. Summarizing,

Definition: *An arrangement A is ρ-decomposable if it is an elementary feature or if exists two ρ-decomposable arrangements B and C with*

- $A = B \cup C, \quad B \cap C = \emptyset$
- $||B| - |C|| \leq 1$
- $\rho(X_B, X_C) \geq \rho$

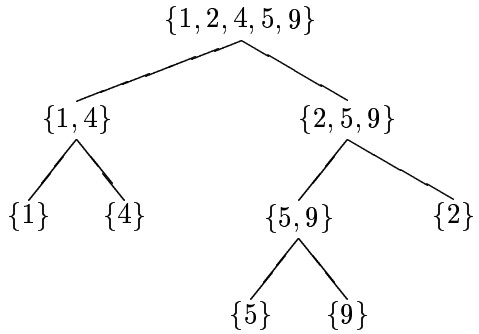

Figure 1: A ρ-decomposable arrangement can be broken down recursively into conjunctions of positively correlated smaller arrangements.

4.3 A Likelihood Bound

In general $P_0(X_A = 1)$ and $P_1(X_A = 1)$ depend on A and decrease as $|A|$ increases. A reasonable assumption for P_0 is some type of exponential decrease, and indeed this is what we observe empirically. On the other hand, if A is a ρ-decomposable arrangement (ρda), we might expect a slower rate of decrease under P_1. In fact, we can show that the rate of decrease is $\rho^{\log_2 k}$. As a result, for "reasonable" values of ρ, $P_1(X_A = 1) \gg P_0(X_A = 1)$ for "large" A. We cannot, however, say anything precise about the likelihood ratio since we do not propose a model for P_0. But we can give a precise lower bound on $P(X_A = 1)$. Let $\mathcal{A}(k, \rho)$ denote the set of all ρda's with $|A| = k$.

THEOREM: *For any $k \geq 1$, $\rho > 0$ and $A \in \mathcal{A}(k, \rho)$,*

$$P_1(X_A = 1) \geq \min_{1 \leq i \leq d} P_1(X_i = 1) \cdot \rho^{\log_2 k}. \tag{1}$$

Sketch of the Proof: Let $\xi = \min_{1 \leq i \leq d} P_1(X_i = 1)$ and write $k = 2^l + j$ where $l \geq 0$ and $0 \leq j < 2^l$. It can be shown by an induction argument on k that

$$P_1(X_A = 1) \geq \xi \cdot \rho^{l + j2^{-l}} \tag{2}$$

Then (2) implies (1) by the concavity of the function $u \to \log_2 u$. The get the flavor of the induction step, suppose (2) is true for $k = 1, 2$ and consider the case $k = 3$. Then $l = j = 1$ and $l + j2^{-l} = \frac{3}{2}$. For binary U, let $v(U) = P_1(U = 1)P_1(U = 0)$, the variance. Let $A = \{a, b, c\}$ and suppose $A \to \{a, b\} \bigcup \{c\}, \{a, b\} \to \{a\} \bigcup \{b\}$ is a ρ-decomposition. Then,

$$\begin{aligned}
P_1(X_a X_b X_c = 1) &\geq P_1(X_a X_b = 1)P_1(X_c = 1) + \rho\left[v(X_a X_b)v(X_c)\right]^{1/2} && (3)\\
&\geq \rho\xi \cdot \xi + \rho\left[\rho\xi(1 - \rho\xi)\xi(1 - \xi)\right]^{1/2} && (4)\\
&\geq \xi^2\rho + \rho\left[\rho\xi^2(1 - \xi)^2\right]^{1/2} && (5)\\
&= \xi\rho^{3/2}. && (6)
\end{aligned}$$

Inequality (3) is due to $\rho(X_a X_b, X_c) \geq \rho$, (4) holds because $x \to x(1 - x)$ is increasing on $0 \leq x \leq 1/2$ and (5) is implied by $\rho\xi \leq \xi$.

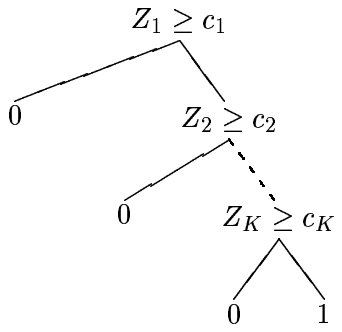

Figure 2: The detector is a coarse-to-fine sequence of filters.

5 The Model Classifier

Detection can be viewed as a sequence of hypothesis tests of increasing complexity relative to the null hypothesis of "background"; each test is applied only when all simpler ones have rejected the null. Since the overwhelming majority of subimages examined are in fact background, the result is a highly coarse-to-fine process in which very few subimages are investigated in detail.

Fix ρ. Each hypothesis test is based on the number $Z_{k,\rho}$ of ρda's of size k present in the picture I:

$$Z_{k,\rho}(I) = \sum_{A \in \mathcal{A}(k,\rho)} X_A(I).$$

Let K be the largest size k which "covers" the object class in the sense that $P_1(Z_{k,\rho} \geq 1) = 1$. (In our experience it never happens that arrangements of size k cover but arrangements of size $j < k$ do not.) Given thresholds $\{c_1, \ldots, c_K\}$, we classify I as object if it contains more than c_k ρda's for each $k = 1, ..., K$. In other words, the classifier is

$$f_\rho(I) = \prod_{k=1}^{K} 1_{\{Z_{k,\rho}(I) \geq c_k\}}.$$

The thresholds $c_1, ..., c_K$ are defined by $c_k = \max\{j : P_1(Z_{k,\rho} \geq j) = 1\}$. That is, they are the maximum values which yield $\alpha(f_\rho) = 0$. We implement f_ρ as a series of filters, as depicted in Figure 2.

Finally, the natural choice of ρ is the value minimizing the false positive error:

$$\rho^* = \arg\min_\rho \beta(f_\rho).$$

However, we have not yet performed any systematic exploration of the possible ρ values; in fact, from here on we assume ρ is fixed. In our experiments we take $\rho = .1$.

6 Learning

In practice we cannot construct f_ρ because we don't have the sets $\mathcal{A}_{k,\rho}, k = 1, ..., K$. They require knowing P_1 and there might be a great many of them. Instead, our experiments

are based on an approximation. We cannot hope to estimate *all* the ρda's, so we attempt to find a fixed number n of these for each size $k \leq K$. Thus, given $\mathcal{L}$, one goal of learning is to estimate a subfamily of $\mathcal{A}_{\mathcal{L}}(k,\rho) \subset \mathcal{A}(k,\rho)$ of size n for each $k \leq K$. The other learning task is to estimate the thresholds $c_1, ..., c_K$.

Whereas the definition of a decomposable arrangement is top-down, the estimation procedure is bottom-up. Correlations are estimated under $\hat{P}_1$, the empirical measure derived from $\mathcal{L}$. The construction is recursive: First build a family $\{X_i X_j\}$, then a family $\{X_i X_j X_k\}$, etc. In order to construct $\mathcal{A}_{\mathcal{L}}(2k,\rho)$ we only need $\mathcal{A}_{\mathcal{L}}(k,\rho)$; and for $\mathcal{A}_{\mathcal{L}}(2k+1,\rho)$ we only need $\mathcal{A}_{\mathcal{L}}(k,\rho)$ and $\mathcal{A}_{\mathcal{L}}(k+1,\rho)$.

Consider the even case. Let $\mathcal{A}'_{\mathcal{L}}(2k,\rho)$ be the set of all arrangements $A_1 \bigcup A_2$ where

- $A_1, A_2 \in \mathcal{A}_{\mathcal{L}}(k,\rho)$;
- $\hat{\rho}(X_{A_1}, X_{A_2}) \geq \rho$;
- $suppX_{A_1} \bigcap suppX_{A_2} = \emptyset$.

Here, $suppX_A = \cup_{i \in A} suppX_i$.

We want to select a subset of $\mathcal{A}'_{\mathcal{L}}(2k,\rho)$ of size n, if possible. Generally, $n \ll |\mathcal{A}'_{\mathcal{L}}(2k,\rho)| \ll n^2$. If $|\mathcal{A}'_{\mathcal{L}}(2k,\rho)| \leq n$, put $\mathcal{A}_{\mathcal{L}}(2k,\rho) = \mathcal{A}'_{\mathcal{L}}(2k,\rho)$. Otherwise, $\mathcal{A}_{\mathcal{L}}(2k,\rho)$ is randomly sampled from $\mathcal{A}'_{\mathcal{L}}(2k,\rho)$, one arrangement at a time, among all those which are present on those training example(s) which are covered by the least number of already chosen arrangements. In other words, the random sampling attempts to maximize the quantity $\min_{\omega \in \mathcal{L}} \left\{ \sum_{A \in \mathcal{A}_{\mathcal{L}}(2k,\rho)} X_A(\omega) \right\}$.

The recursive process is initialized with $\mathcal{A}'_{\mathcal{L}}(1,\rho)$, the n most common elementary tests, and terminates at the first k for which it is no longer possible to cover the object examples with n arrangements of size k.

Finally, the natural estimators of the thresholds $c_1, ..., c_K$ are

$$\hat{c}_k = max \left\{ c : \hat{P}_1 \left(\sum_{A \in \mathcal{A}_{\mathcal{L}}(\rho,k)} X_A \geq c \right) = 1 \right\}, \quad k = 1, ..., K.$$

Clearly, this over-estimates c_k, in fact rather severely in many cases. Therefore, we take one-half this value in all our experiments; this yields $\alpha(f) = 0$, a fundamental constraint in our formulation.

7 Experiments with Wings

The experiment was designed to exaggerate problem of "clutter" - background structures which resemble the targets. We also wanted to evaluate the proposed detector and the learning algorithm in a controlled statistical setting. This means that $\mathcal{L}$ is truly a random sample from P_1 and that the error rates $\alpha(f)$ and $\beta(f)$ of any proposed classifier, including maximum likelihood, can be estimated to high precision.

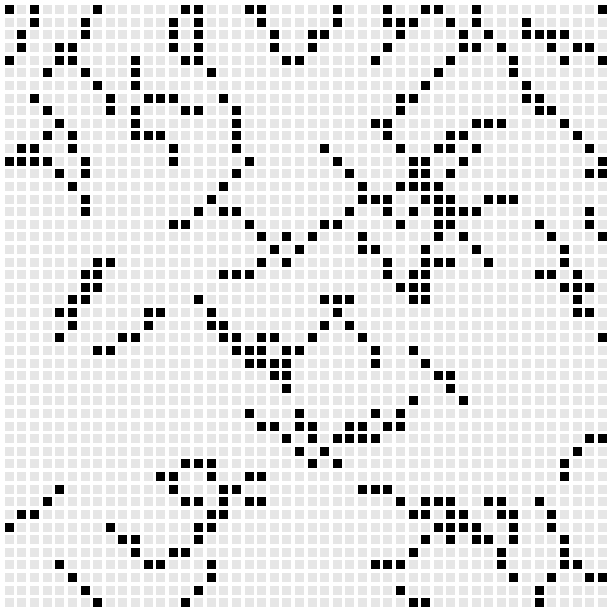

Figure 3: A "wing world" scene.

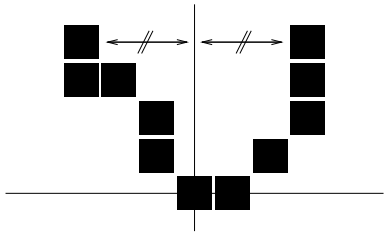

Figure 4: "Wings" consist of two random lines of equal length starting from a common pixel.

7.1 Scenes

"Scenes" are binary and composed entirely of short, jagged lines; see Figure 3. The lines ("clutter") are realizations of random walks; the transition probabilities orient the segments either northwest or northeast. Scenes are then generated as follows: Randomly choose a set of locations $x_1, x_2, \ldots$ in the integer lattice, then randomly choose a direction, either NW or NE, for each location x_i and generate a random walk of length m starting at x_i. In the NW case, the walk proceeds either W, NW or N with probabilities $\frac{1}{4}, \frac{1}{2}, \frac{1}{4}$ respectively; in the NE case these directions are N, NE or E. The locations of the vertex of the "wings" are also randomly selected. Wings consist of two diagonal lines, one NW and one NE, starting from the same pixel and constrained by the symmetry condition illustrated in Figure 4.

The detection problem is difficult because every object instance is a distinguished configuration of two instances of clutter. Wings and background are inseparable based solely on local features; long-range correlations must be taken into account. On the other

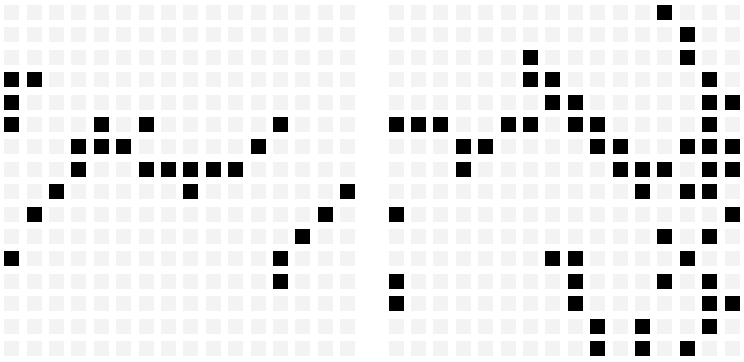

Figure 5: Left: A wing subimage from the training set. Right: A background subimage.

hand, it is not necessary to consider very dense representations, such as a complete wing template, since a few black pixels oriented NW or NE already give ample evidence for a line segment. Finally, it is by no means obvious how a learning algorithm can "discover" the symmetry constraint or accommodate the large variation among wing instances.

7.2 Training and Testing

We generated a large scene and randomly extracted 1000 16×16 subimages centered at wing locations; thus $|\mathcal{L}| = 1000$. The optimal error rate seems to be around 2%, obtained by knowing the model geometry and checking for two diagonal lines which have the correct length and verify the symmetry constraint at the endpoints. This describes the maximum likelihood classifier

$$f_{ML}(I) = I_{\{P_1(I) > P_0(I)\}}$$

because $P_1(I) > P_0(I)$ for any wing subimage I and because $P_1(I) = 0$ for any background subimage. Since every wing is found, the errors are all false positives.

In our classifier, the elementary tests are not the individual pixels, black or white. Instead, they are edge-based. "Edges" are two black pixels diagonally adjacent. Every elementary test X_i has a location x_i in the 16×16 grid and an orientation $\theta_i \in \{NW, NE\}$; $X_i = 1$ if there is an oriented edge of type θ_i anywhere in a 2×2 neighborhood of x_i. Such tests make the classifier stable with respect to small perturbations of the wing shape, but still precise enough to exploit the symmetry property.

The arrangements which are estimated from $\mathcal{L}$ accumulate on the wings and capture their shape. For small A the locations are usually confined to one side, but for larger A the longer range dependencies are exploited and A contains pixels on both lines. And the probability distributions of the random variables Z_k under P_0 and P_1 are indeed quite separated; the shapes of the cumulative distribution functions look rather similar to those for faces, shown in Figure 7. Finally, the best *combined* error rate we achieve is $\alpha + \beta \approx .07$; it is somewhat higher if we implement the constraint that $\alpha = 0$. In our view, separating these two populations is very difficult. For example, nearest-neighbors works poorly, even with "smart" (e.g., invariant) metrics.

8 Experiments with Faces

The pose is characterized by a triangle whose vertices are the positions of the two eyes and the mouth. Since our goal is to detect upright, frontal views of faces, the triangles point down and are basically isosceles. There are then five degrees of (linear) freedom: two for location, and one each for orientation, scale (e.g., the distance between the eyes) and elongation (e.g., the height-to-width ratio). We do not search for faces at all scales simultaneously. Rather, we first assume that all faces are within about $\pm 25\%$ of a minimal reference scale and then find the larger ones by re-running the algorithm on downsampled scenes.

The triangles are recursively partitioned. There is one learning problem per partition, but the algorithm is the same; only the training set changes. For example, we might first group together all poses whose location falls in a particular 4×4 window. The corresponding training set is then quite heterogeneous since all the scales, orientations and elongations are mixed together and the location is only approximate. The first step in processing the scene would then be to evaluate the resulting classifier f on the subimage I around each non-overlapping window. Only the pixels in windows for which $f(I) = 1$ would be retained as possible face locations. Naturally, there are many false alarms because only simple, sparse arrangements can cover the training ensemble. However even a false positive rate of 50% means that half the scene is finished with very elementary processing, perhaps involving only arrangements of size one (i.e., edge statistics).

The next division might divide scales into "small" and "large." This leads to two new, more restricted, learning problems. (Actually, it is enough to "expand" the arrangements learned for the small scale.) The training set is now more homogeneous and hence larger, more discriminating arrangements are found. We continue in this way, steadily restricting the amount of variation in the triangles. Eventually we might constrain the location to a 2×2 window and pin all other the parameters at one "reference pose" (triangle shape). In some sense, the limit of this process is a very global classifier, such as a deformable template [1], which might involve on-line optimization in order to refine nonlinear aspects of the pose and allow for face *recognition*.

8.1 Training Set

We will illustrate learning by fixing the shape of the triangle and locating it anywhere in a 4×4 window; as indicated above, this might be followed by further restricting the location.

The training set $\mathcal{L}$ is constructed from the Olivetti database of faces, which has ten frontal poses for each of forty individuals. After downsampling, each of these 400 pictures is 46×56 and we mark the locations of the eyes and mouth; there is relatively more variation in the scale and elongation of the triangles than in their orientation. We use 300 pictures (30 individuals) for training and the rest for estimating the false negative rate.

Recall that the direct input to the classifier is the feature vector of elementary tests $\{X_i\}$, not the original grey level image, and that each X_i corresponds to a localized, oriented edge as described in Section 4.1. Hence, for each training image we compute an edge array which has four boolean features at each pixel corresponding to horizontal and

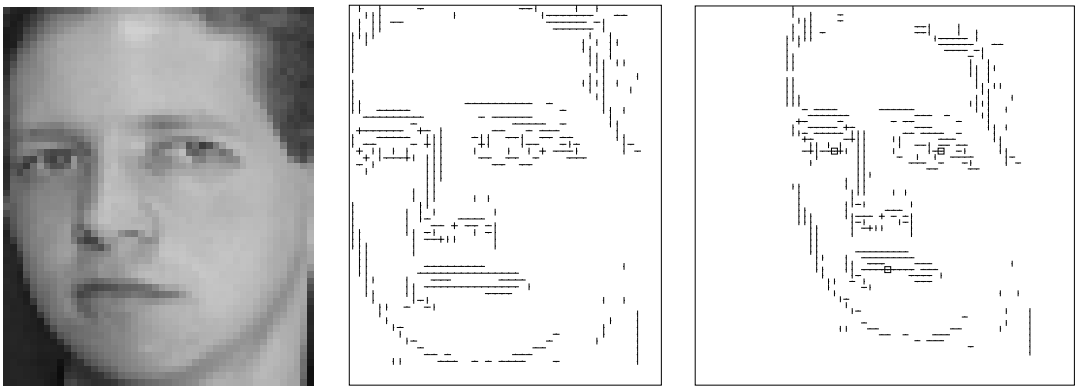

Figure 6: Left: A face training image. Middle: The extracted edges. Right: The registered edge map (right); the three small squares indicated the reference pose.

vertical edges, and two polarities. Each of these edge arrays is then transformed by an affine mapping which carries the original triangle to the reference one. In other words, the eyes and the mouth are sent to fixed locations. In Figure 6 we show one greyscale picture (left) in the training set together with the original (middle) and transformed (right) edge maps. The training database then has $300 \times 4^2 = 4800$ registered edge maps; the elementary tests are local (2×2) disjunctions of these maps.

8.2 Learned Arrangements

Shown in Figure 7 are two arrangements learned from $\mathcal{L}$, one of size six and one of size eight. The orientations and polarities of the participating edges are indicated by the small strips. Clearly the lefthand arrangement captures information about the face contour, whereas the righthand one reflects typical correlations among edges above the eyes and in the mouth. The lefthand arrangement splits into two subarrangements of size three, one on each side of the face, and each of these divides into a single edge and a two paired edges. These arrangements are quite "typical" of the thousands made. In fact, it turns out that all the arrangements are composed of edges around the eyes, nose, mouth and forehead outline. This is illustrated in Figure 8 in which the darkness of a pixel is proportional to the number of times an edge whose support involves that pixel appears in any of the learned arrangements.

One measure of the discriminating power of the arrangements is illustrated in Figure 9. The vertical axis indicates probability and the horizontal axis indicates arrangement size. The curve is the theoretical lower bound in (1). We only use elementary tests with P_1-values approximately one-half or higher, so that $\min_{1 \le i \le d} X_i \approx 0.5$ in (1). The value taken for ρ is .3; see Section 8.3. Thus the curve is $k \to .5(.3)^{\log_2 k}$. We randomly sampled ten arrangements A for each $k = 1, ..., 7$ and computed the probabilities of the events $\{X_A = 1\}$ under both P_0 and P_1; these are indicated, respectively, by the +'s and the $\diamond$'s. As can be seen, the actual likelihoods on faces lie considerably above the bound.

Finally, Figure 10 depicts the cumulative distribution functions, $P_0(Z_k \le z)$ and $P_1(Z_k \le z)$, as estimated from data, for $k = 3$ and $k = 4$. As seen again, ρda's of

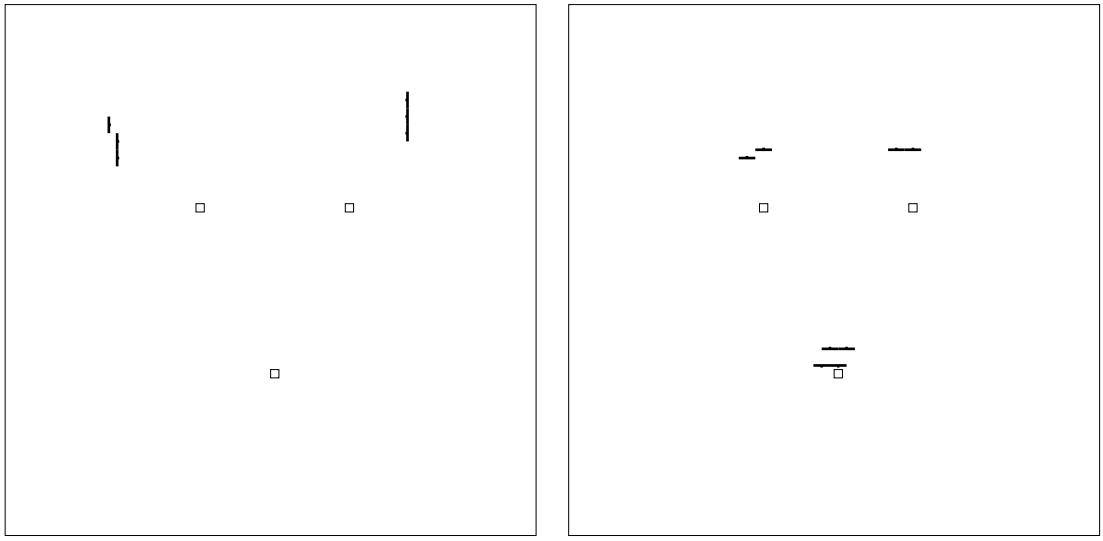

Figure 7: Examples of arrangements of sizes 6 and 8 on faces.

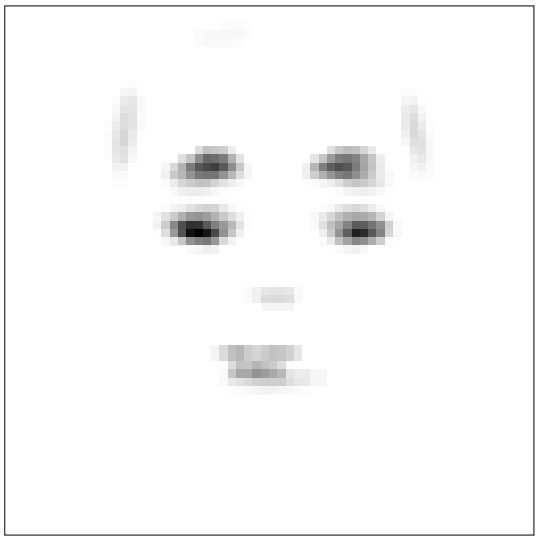

Figure 8: Areas of the face appearing in the arrangements; dark indicates high usage.

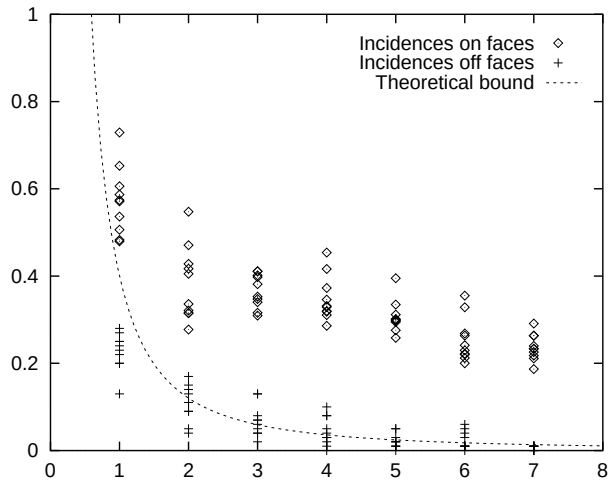

Figure 9: The likelihoods of a sample of learned arrangements of sizes $k = 1, ..., 7$ on faces ($\diamond$) and off faces ($+$). The curve is the theoretical lower bound on faces.

modest size are extremely rare under P_0 but not under P_1. Hence, for example, face and background subimages are separated rather well by Z_4.

8.3 Correlation Estimates

Are the ρda's estimated from $\hat{P}_1$ actually ρ-decomposable with respect to P_1? Some are not and some are decomposable at even a higher level. Let $\rho_0 = .1$; this is the value used in our experiments. Recall that each constructed $A \in \mathcal{A}_{\mathcal{L}}(k, \rho_0)$ has a *proposed* ρ_0-decomposition. One can then use additional data (e.g., the test set) to check this decomposition by re-estimating the correlations.

In fact, we can determine $\rho_{max}(A)$, the maximal value of ρ for which the given decomposition of A is a ρ-decomposition. This value may be smaller or larger than ρ_0. The results, shown in Figure 11, are conservative because checking whether $A \in \mathcal{A}(k, \rho_0)$, i.e., whether there is *any* ρ_0-decomposition of A, would lead to larger levels and shift the curve in Figure 11 to the right. We find, for example, that the decompositions for about 95% of the arrangements are valid at $\rho > 0$, 80% at $\rho \geq .1$ (the target value) and 45% at $\rho \geq .2$.

8.4 Estimated Error Rates

Error rates are difficult to estimate, especially without analyzing full scenes. To keep the paper self-contained and in the framework of statistical learning we simply classified the remaining 100 faces in the original database after registering them in the same fashion as the training images, and also a random sample of 46×56 subimages extracted from various greylevel scenes taken from the WWW. In [7] more realistic estimates are reported based on searching for faces in large scenes, with false positive rates expressed by the number of false alarms per pixel, as in [3].

Due to the conservative placement of the thresholds $c_1, ..., c_K$, the false negative rate is indeed zero. The false positive error as a function of the feature complexity, i.e., $\beta_k =$

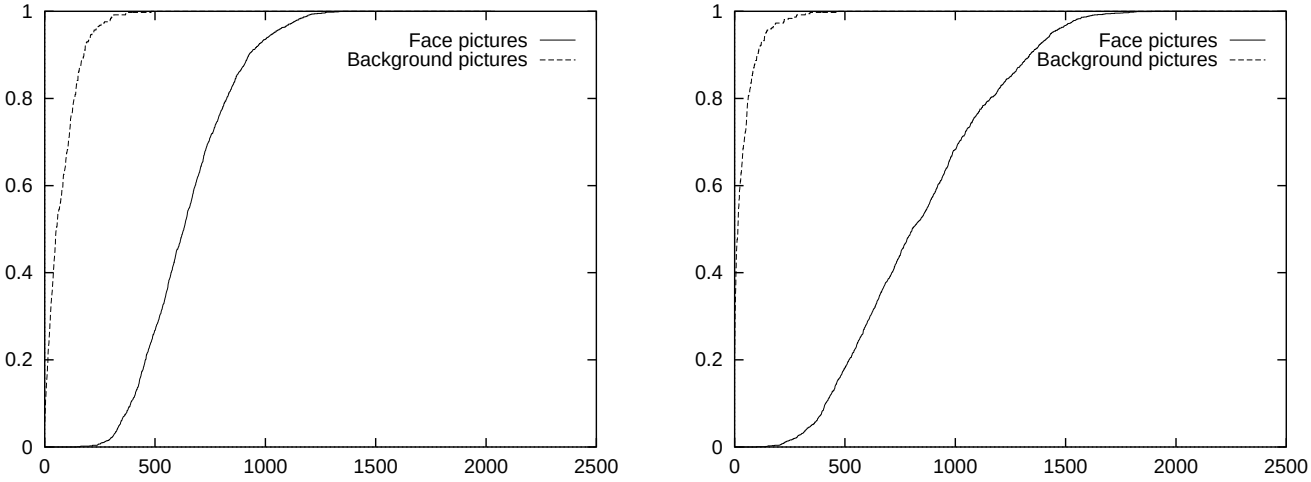

Figure 10: Distribution functions of Z_3 and Z_4 on faces

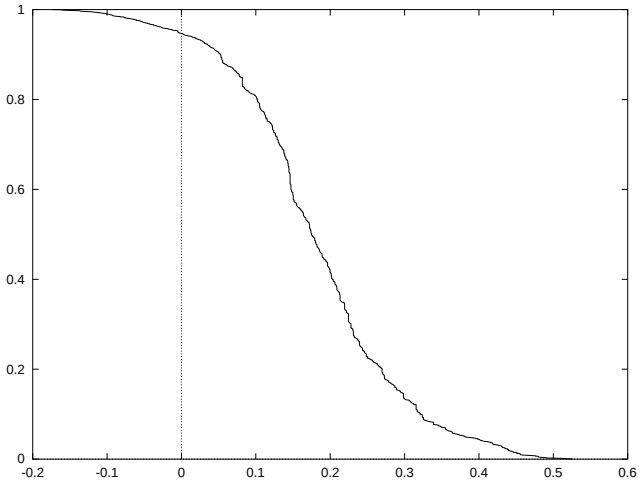

Figure 11: Proportion of the learned decompositions which are actually decomposable at level ρ.

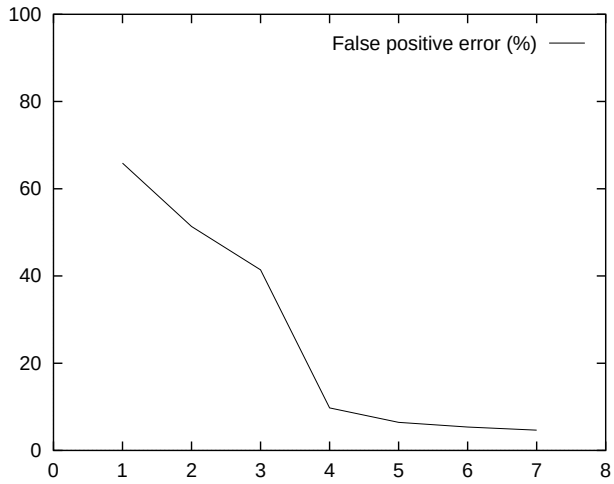

Figure 12: The false positive error as a function of the size of the arrangement.

$\hat{P}_0(Z_1 \geq c_1, ..., Z_k \geq c_k)$, is given in Figure 12. The important property is the sharp decrease with k; the final value (approximately 4%) is relatively meaningless since this is but one step in a coarse-to-fine process. For example, if we restrict the location to a 2×2, the rate drops to well below one percent.

9 Conclusion

We have formulated object detection as a learning problem constrained by invariance and efficiency. Our basic assumption is that it is ultimately possible to detect objects by discovering features which are considerably more likely under the "object distribution" than under the "background distribution."

Although the context is statistical and inductive, we have not appealed to a *general* theory of inductive learning, for instance structural risk minimization [15], or to theoretical results about neural network classifiers [4],[6], or to generic representations, such as Bayes nets. *Instead, the learning is highly dedicated to the vision problem.* We capture the spatial dependency structure by estimating correlations among conjunctions of localized features. Each estimated parameter has an explicit interpretation, which makes training very fast. And we *directly* address the natural constraints - invariance to photometric and geometric distortions, very low false negative error and limited amounts of training data.

We have concentrated on a two-dimensional pattern and not a three-dimensional object. (We place the frontal views of faces in the former category.) It remains to be seen whether the methodology can be extended to handle all the degrees of freedom in imaging a 3D object. Obviously, simultaneously detecting many different object classes $c = 1, ..., C$ is still more difficult. In our framework, the key question is "reusable parts" - how the size of the combined feature set $\bigcup_{c=1,...,C} \mathcal{A}_c(k)$ scales with C, where $\mathcal{A}_c(k)$ is the set of arrangements of size k dedicated to object c. We want logarithmic scaling, resulting from representing different objects with the same arrangements whenever possible.

Finally, in defense of limited goals, nobody has yet demonstrated that objects from

even one generic class under constrained poses can be rapidly detected without errors in complex, natural scenes; visual selection by humans occurs within two hundred milleseconds and is virtually perfect.

References

[1] Y. Amit. *Deformable template methods for object detection.* Tutorial, ICIP '98, Chicago, 1998.

[2] Y. Amit and D. Geman. Shape quantization and recognition with randomized trees. *Neural Computation*, 9:1545–1588, 1997.

[3] Y. Amit and D. Geman. A computational model for visual selection. *Neural Computation*, 1999. To appear.

[4] E. B. Baum and D. Haussler. What size net gives valid generalization? *Neural Comp.*, 1:151–160, 1989.

[5] T. F. Cootes and C. J. Taylor. Locating faces using statistical feature detectors. In *Proceedings, Second International Conference on Automatic Face and Gesture Recognition*, pages 204–209. IEEE Computer Society Press, 1996.

[6] L. Devroye. *Probabilistic methods for pattern recognition.* Springer-Verlag, Berlin, 1995.

[7] F. Fleuret and D. Geman. Coarse-to-fine face detection. Technical report, INRIA-Rocquencourt, 1999. In preparation.

[8] D. Geman and B. Jedynak. An active testing model for tracking roads from satellite images. *IEEE Trans. PAMI*, 18:1–15, 1996.

[9] B. Jedynak and F. Fleuret. 3d object recognition from geometric queries. In *Proc. Image'Com 96*, Bordeaux, France, 1996.

[10] T. Leung, M. Burl, and P Perona. Finding faces in cluttered scenes using labeled random graph matching. In *Proceedings, 5th Int. Conf. on Comp. Vision*, pages 637–644, 1995.

[11] E. Osuna, R. Freund, and F. Girosi. Training support vector machines: an application to face detection. In *Proceedings, CVPR*, pages 130–136. IEEE Computer Society Press, 1997.

[12] H. A. Rowley, S. Baluja, and K. Takeo. Neural network-based face detection. *IEEE Trans. PAMI*, 20:23–38, 1998.

[13] K. K. Sung and T. Poggio. Example-based learning for view-based face detection. *IEEE Trans. PAMI*, 20:39–51, 1998.

[14] S. Ullman. *High-Level Vision.* M.I.T. Press, Cambridge, MA., 1996.

[15] V. Vapnik. *The Nature of Statistical Learning.* Springer-Verlag, Berlin, 1996.

[16] K. Wilder. *Decision tree algorithms for handwritten digit recognition.* PhD thesis, University of Massachusetts, Amherst, Massachusetts, 1998.

[17] A. L. Yuille, D. S. Cohen, and P. Halliman. Feature extraction from faces using deformable templates. *Inter. J. Comp. Vision*, 8:104–109, 1992.